CKM PARAMETERS FROM $|\Delta S| = 1$ PROCESSES*

G. Valencia

Department of Physics, Iowa State University
Ames IA 50011, USA

(Received September 27, 2002)

I briefly review how measurements in rare kaon decays and in hyperon decays will help unravel the CKM mixing angles. I then discuss recent work in selected kaon decay modes and in estimates for CP violation in non-leptonic hyperon decay.

PACS numbers: 12.39.Fe, 12.40.Vv, 13.20.Eb, 13.25.Es

1. Introduction

As we have already seen in the lectures by Jarlskog [1], the CKM matrix is a unitary 3×3 matrix with four independent parameters [2]. In the commonly used, approximate, parameterization of Wolfenstein [3] it is written as,

$$V = \begin{pmatrix} V_{ud} & V_{us} & V_{ub} \\ V_{cd} & V_{cs} & V_{cb} \\ V_{td} & V_{ts} & V_{tb} \end{pmatrix} \tag{1}$$

$$V \approx \begin{pmatrix} 1-\lambda^2/2 & \lambda & A\lambda^3(\rho - i\eta) \\ -\lambda & 1-\lambda^2/2 & A\lambda^2 \\ A\lambda^3(1-\rho-i\eta) & -A\lambda^2 & 1 \end{pmatrix} . \tag{2}$$

Of course, the parameter $\lambda \approx V_{us}$ is extracted from $|\Delta S| = 1$ transitions, both from semi-leptonic kaon decay $K \to \pi e \nu$ and from semi-leptonic hyperon decay $\Lambda \to p e \nu$ [4]. The parameter $A \approx V_{cb}/\lambda^2$ is extracted from B decay, and the other two parameters ρ and η which give information on V_{ub} and V_{td} are the focus of intense studies to test the CKM structure in

* Presented at the XLII Cracow School of Theoretical Physics, Zakopane, Poland May 31–June 9, 2002.

the standard model. The latest numbers quoted by the Particle Data Book are [5],

$$
\begin{aligned}
\rho &= 0.22 \pm 0.10\,, \\
\eta &= 0.35 \pm 0.05\,.
\end{aligned} \tag{3}
$$

Since these two parameters involve ub or td transitions, their appearance in $|\Delta S| = 1$ processes must arise at the one-loop level. This can be easily seen from the one-loop flavor-changing neutral current in the $|\Delta S| = 1$ sector, schematically shown in the diagrams of figure 1, where V_{td} is seen to enter via the top-quark intermediate state.

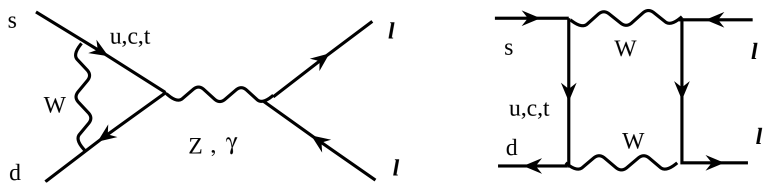

Fig. 1. One-loop diagrams responsible for $|\Delta S| = 1$ transitions in the Standard Model in channels with a lepton anti-lepton pair.

In figure 2 we illustrate how some of the rare kaon decays generated by standard model diagrams as in figure 1 contribute to the knowledge of the unitarity triangle. In particular, I show schematically the usual unitarity triangle (dashed) and the contributions that kaon measurements could provide (solid).

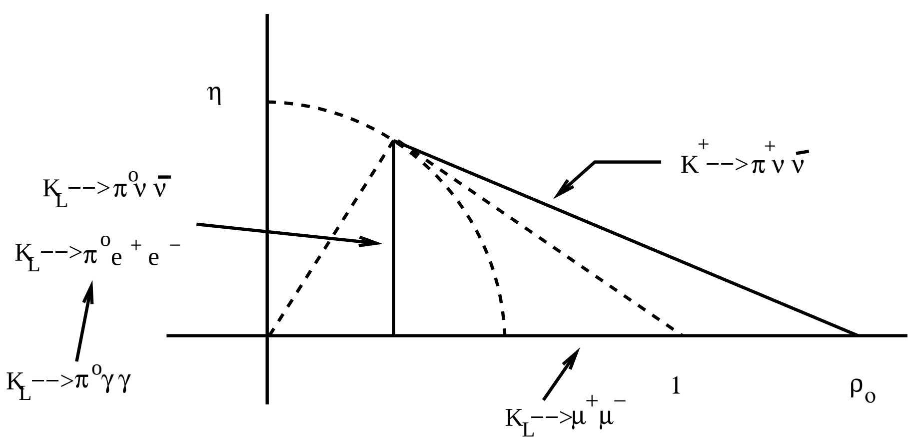

Fig. 2.

It is convenient to divide the kaon decay modes into the following three types.

- There are extremely clean modes with small theoretical uncertainties. They always involve a $\nu\bar{\nu}$ pair in the final state. The two most commonly discussed modes of this type are $K^+ \to \pi^+\nu\bar{\nu}$ and $K_{\rm L} \to \pi^0\nu\bar{\nu}$ [6,7]. Modes with additional pions in the final state have also been discussed in the literature [8].

  As illustrated in figure 2, $K^+ \to \pi^+\nu\bar{\nu}$ provides a measurement of the diagonal of the solid triangle. Within the standard model one finds [7],

  $$B(K^+ \to \pi^+\nu\bar{\nu}) \approx 1.0 \times 10^{-10} A^4(\eta^2 + (\rho_0 - \rho)^2)\,, \tag{4}$$

  where $\rho_0 \approx 1.4$ is a parameter that roughly speaking measures the importance of charm as an intermediate state [7].

  The experimental status of this mode is that BNL 787 has seen two events from which they derive [9]

  $$B(K^+ \to \pi^+\nu\bar{\nu})_{\rm exp} = (1.57^{+1.75}_{-0.82}) \times 10^{-10}\,. \tag{5}$$

  Another mode of this type is $K_{\rm L} \to \pi^0\nu\bar{\nu}$ which measures the vertical side of the solid triangle, or the CP-violating phase η. Within the Standard Model the expectation is [7]

  $$B(K_{\rm L} \to \pi^0\nu\bar{\nu}) \approx 4.1 \times 10^{-10} A^4\eta^2\,. \tag{6}$$

  This mode has not been seen experimentally although there are a couple of proposals that may eventually measure this mode. There is an upper bound from KTeV [10] $B(K_{\rm L} \to \pi^0\nu\bar{\nu}) < 5.9 \times 10^{-7}$ and a theoretical upper bound derived from the charged mode and a minimal set of assumptions about the nature of the CP-violating interactions [11] $B(K_{\rm L} \to \pi^0\nu\bar{\nu}) < 1.7 \times 10^{-9}$.

- The second type consists of modes with charged leptons in the final state. These modes suffer from long distance electromagnetic effects and are less clean theoretically. Examples of this kind are $K_{\rm L} \to \mu^+\mu^-$ which could measure the horizontal side of the solid triangle in figure 2 if one could subtract the long distance effects [12]. A second example is $K_{\rm L} \to \pi^0 e^+e^-$ which could measure the parameter η if its different components can be un-tangled. In my talk I will discuss the CP conserving component of the latter, which proceeds via a two-photon intermediate state. I will also discuss in detail the related mode $K_{\rm L} \to \pi^0\gamma\gamma$ with emphasis on recent theoretical and experimental developments.

- Finally, the purely hadronic modes such as $K \to \pi\pi$ from which the parameter ε' is extracted, suffer from large theoretical uncertainties associated with non-perturbative QCD effects. In my second talk I will discuss $\Lambda \to p\pi^-$ in connection with the efforts by Fermilab experiment E871 to observe CP violation in hyperon decay. This mode is also plagued with large theoretical uncertainty.

2. $K_{\rm L} \to \pi^0\gamma\gamma$

This reaction is interesting for two reasons. One is that it mediates a CP conserving background to $K_{\rm L} \to \pi^0 e^+e^-$ and thus it must be understood if one hopes to extract useful short distance information from the latter. A detailed discussion of this can be found in the many reviews on the subject [6]. As I will discuss in this talk, the mode $K_{\rm L} \to \pi^0\gamma\gamma$ has two invariant amplitudes that roughly correspond to the photon pair being in an S or D wave. The state with two-photons in an S-wave leads to a negligible CP conserving $K_{\rm L} \to \pi^0 e^+e^-$, proportional to m_e^2, whereas the state with two-photons in a D-wave can yield a sizable CP conserving $K_{\rm L} \to \pi^0 e^+e^-$. This provides a strong motivation for a detailed study of the $K_{\rm L} \to \pi^0\gamma\gamma$ spectrum. A second reason why this reaction is of interest is as a test of chiral perturbation theory which makes an unambiguous prediction at leading order (p^4).

The framework of χPT has proved extremely useful for analyzing low energy processes involving the pseudoscalar meson octet and photons. At low energies, the strong and electromagnetic interactions of these particles can be adequately described with a chiral Lagrangian with up to four derivatives. The most general chiral Lagrangian to this order has been written down by Gasser and Leutwyler [13]. It consists of two terms at leading order, $\mathcal{O}(p^2)$:

$$\mathcal{L}_S^{(2)} = \frac{f_\pi^2}{4}{\rm Tr}(D_\mu\Sigma D^\mu\Sigma^\dagger) + B_0\frac{f_\pi^2}{2}{\rm Tr}(M\Sigma + \Sigma^\dagger M). \tag{7}$$

M is the diagonal matrix (m_u, m_d, m_s), and the meson fields are contained in the matrix $\Sigma = \exp(2i\phi/f_\pi)$ with:

$$\phi \;=\; \frac{1}{\sqrt{2}}\begin{pmatrix} \pi^0/\sqrt{2}+\eta/\sqrt{6} & \pi^+ & K^+ \\ \pi^- & -\pi^0/\sqrt{2}+\eta/\sqrt{6} & K^0 \\ K^- & \overline{K^0} & -2\eta/\sqrt{6} \end{pmatrix} \tag{8}$$

Σ transforms under the chiral group as $\Sigma \to R\Sigma L^\dagger$. For processes in which photons are the only external fields the covariant derivative is given by,

$$D_\mu\Sigma = \partial_\mu\Sigma - ieA_\mu[Q,\Sigma] \tag{9}$$

and Q is the diagonal matrix $(-2/3, 1/3, 1/3)$.

At next to leading order, $\mathcal{O}(p^4)$, there are ten new operators [13], none of which contributes to $K_{\rm L} \to \pi^0\gamma\gamma$ at order p^4.

For $|\Delta S| = 1$ processes we also need the weak interactions. In the standard model, the dominant $|\Delta S| = 1$ operators in the effective weak Hamiltonian transform as $(8_{\rm L}, 1_{\rm R})$ under chiral rotations. We can write a chiral representation for operators with this transformation property, and once again organize them in terms of the number of derivatives. The lowest order Lagrangian constructed in this way contains two derivatives [14]:

$$\mathcal{L}_{\rm W}^{(2)} = \frac{G_{\rm F}}{\sqrt{2}}|V_{ud}V_{us}^*|g_8 {\rm Tr}(\lambda_6 L_\mu L^\mu)\,, \tag{10}$$

where $L_\mu = if_\pi^2 \Sigma D_\mu \Sigma^\dagger$. The constant is fit from $K \to \pi\pi$ decays, $g_8 \sim 5.1$. It is conventional to use the combination of constants,

$$G_8 \equiv \frac{G_{\rm F}}{\sqrt{2}}|V_{ud}V_{us}^*|g_8 \approx 9.1 \times 10^{-6}~{\rm GeV}^{-2}. \tag{11}$$

The situation at next to leading order is much more complicated: a very large number of operators, and therefore of unknown coupling constants, has been identified [15]. However, one can explicitly check that none of these contributes at tree-level to $K_{\rm L} \to \pi^0\gamma\gamma$. This implies that the one-loop result has to be finite as there are no counterterms at order p^4 that can be used to absorb divergent terms. Explicit calculation involving diagrams such as the one shown in figure 3, confirms that the one-loop expression is finite. For this reason there is a unique, parameter free, lowest order prediction for this mode from chiral perturbation theory.

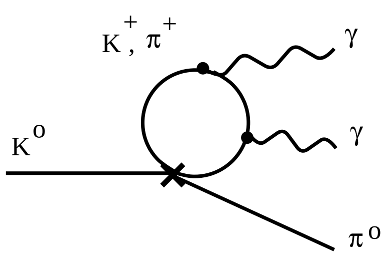

Fig. 3. Example of one-loop diagram generating $K_{\rm L} \to \pi^0\gamma\gamma$ at order p^4. The X indicates a lowest order weak vertex and the circle indicates a lowest order meson–photon vertex.

It has been known since the first experimental results appeared [16] that lowest order (p^4) chiral perturbation theory is not sufficient to explain simultaneously the observed rate and spectrum and that the failure is significant.

For this reason higher order corrections were incorporated into the theoretical prediction early on. For some time now, it has become standard to use a theoretical description which incorporates certain non-analytic terms at next to leading order (p^6) [17, 18], as well as one parameter, a_V [18]. This parameter arises in vector meson dominance models for this decay [19], but it is not the only one. Instead, at order p^6 the amplitude is described by three independent parameters: α_1, α_2 and β in the notation of Cohen *et al.* [18].

The most general form of the $K \to \pi\gamma\gamma$ amplitude contains four independent invariant amplitudes A, B, C and D and can be found in the literature [20]. For the case of $K_{\rm L} \to \pi^0\gamma\gamma$, and in the limit of CP conservation, only two of these amplitudes come into play:

$$\begin{aligned}\mathcal{M}(K_{\rm L}(p_K) \to \pi^0(p_\pi)\gamma(q_1)\gamma(q_2)) &= \frac{G_8\alpha}{4\pi}\varepsilon_\mu(q_1)\,\varepsilon_\nu(q_2) \\ &\Bigg[A\;(q_2^\mu q_1^\nu - q_1\cdot q_2\, g^{\mu\nu}) + 2\frac{B}{m_K^2}\;(p_K\cdot q_1\, q_2^\mu p_K^\nu \\ &+p_K\cdot q_2\, q_1^\nu p_K^\mu - q_1\cdot q_2\, p_K^\mu p_K^\nu - p_K\cdot q_1\, p_K\cdot q_2\, g^{\mu\nu})\Bigg],\end{aligned} \tag{12}$$

In chiral perturbation theory with terms of order up to p^6, the amplitudes A and B take the form [18]:

$$\begin{aligned}A(z) &= 4F\left(\frac{z}{r_\pi^2}\right)\frac{a_1(z)}{z} + 4\frac{F(z)}{z}(1+r_\pi^2-z) \\ &+\frac{a_2 M_K^2}{\Lambda_\chi^2}\left\{\frac{4r_\pi^2}{z}F\left(\frac{z}{r_\pi^2}\right) + \frac{2}{3}\left(2+\frac{z}{r_\pi^2}\right)\left[\frac{1}{6}+R\left(\frac{z}{r_\pi^2}\right)\right] - \frac{2}{3}\log\frac{m_\pi^2}{M_\rho^2}\right. \\ &-2\frac{r_\pi^2}{z^2}(z+1-r_\pi^2)^2\left[\frac{z}{12r_\pi^2}+F\left(\frac{z}{r_\pi^2}\right)+\frac{z}{r_\pi^2}R\left(\frac{z}{r_\pi^2}\right)\right] \\ &\left.+\,8\frac{r_\pi^2}{z^2}y^2\left[\frac{z}{12r_\pi^2}+F\left(\frac{z}{r_\pi^2}\right)+\frac{z}{2r_\pi^2}F\left(\frac{z}{r_\pi^2}\right)+3\frac{z}{r_\pi^2}R\left(\frac{z}{r_\pi^2}\right)\right]\right\} \\ &+\alpha_1(z-r_\pi^2)+\alpha_2, \\ B(z) &= \frac{a_2 M_K^2}{\Lambda_\chi^2}\left\{\frac{4r_\pi^2}{z}F\left(\frac{z}{r_\pi^2}\right)+\frac{2}{3}(10-\frac{z}{r_\pi^2})\left[\frac{1}{6}+R\left(\frac{z}{r_\pi^2}\right)\right]\right. \\ &\left.+\,\frac{2}{3}\log\frac{m_\pi^2}{m_\rho^2}\right\}+\beta\,,\end{aligned} \tag{13}$$

where we use the standard kinematic variables

$$z = \frac{(q_1 + q_2)^2}{M_K^2}, \quad y = \frac{p_K \cdot (q_1 - q_2)}{M_K^2}, \tag{14}$$

and $\Lambda_\chi \approx 4\pi f_\pi \approx 1.17$ GeV.

This form for the two amplitudes does not correspond to a complete calculation in chiral perturbation theory at order p^6. It contains the complete one-loop calculation of order p^4 [21] and two types of terms of order p^6. The first type consists of the non-analytic terms in Eq. (13) that multiply the factors a_2 and $a_1(z)$. The inclusion of these terms is inspired by dispersion relations, and they originate in p^4 corrections to the $K \to 3\pi$ amplitudes [15,22]. The relevant constants which enter a_1 and a_2 are extracted from an analysis of $K \to 3\pi$ data. The second type of term consists of the analytic terms that arise from tree-level contributions from order p^6 chiral Lagrangians. From the analysis of $K \to 3\pi$ in Ref. [15], we have

$$\begin{aligned} a_1(z) &= 0.38 + 0.13 Y_0 - 0.0059 Y_0^2, \\ Y_0 &= \frac{(z - r_\pi^2 - \frac{1}{3})}{r_\pi^2}, \\ a_2 &= 6.5\,, \end{aligned} \tag{15}$$

with $r_\pi = m_\pi / M_K$. The loop form factors are given by [18]

$$\begin{aligned} F(z) &= 1 - \frac{4}{z}\left[\arcsin\left(\frac{1}{2}\sqrt{z}\right)\right]^2, \qquad z \le 4, \\ &= 1 + \frac{1}{z}\left(\log\frac{1-\sqrt{1-4/z}}{1+\sqrt{1-4/z}} + i\pi\right)^2, \qquad z \ge 4, \\ R(z) &= -\frac{1}{6} + \frac{2}{z}\left[1 - \sqrt{4/z - 1}\arcsin\left(\frac{1}{2}\sqrt{z}\right)\right], \qquad z \le 4, \\ & -\frac{1}{6} + \frac{2}{z} + \frac{\sqrt{1-4/z}}{z}\left(\log\frac{1-\sqrt{1-4/z}}{1+\sqrt{1-4/z}} + i\pi\right), \qquad z \ge 4. \end{aligned}$$

The three parameters $\alpha_{1,2}$ and β are related to the three Lorentz invariant couplings that can be derived from a chiral Lagrangian at order p^6. In the following form it is easy to see that there are three possible couplings,

$$\begin{aligned} \mathcal{L} &= \frac{G_8 \alpha_{\rm EM}}{4\pi}\left(c_1 K_{\rm L} \pi^0 F^{\mu\nu} F_{\mu\nu} + \frac{c_2}{M_K^2}\partial^\alpha K_{\rm L} \partial_\alpha \pi^0 F^{\mu\nu} F_{\mu\nu} \right. \\ & \left. + \frac{c_3}{M_K^2}\partial_\alpha K_{\rm L} \partial^\beta \pi^0 F^{\alpha\mu} F_{\mu\beta}\right), \end{aligned} \tag{16}$$

they are related to the parameters we are using by,

$$\begin{aligned}\alpha_1 &= -2c_2 + \frac{c_3}{2}, \\ \alpha_2 &= 4c_1 + 2c_2 + \frac{c_3}{2}, \\ \beta &= -c_3\,. \end{aligned} \tag{17}$$

In the analysis of Ref. [18] the three unknown constants were fixed in terms of the contribution they receive from vector-meson exchange, supplemented with a minimal subtraction *Ansatz*:

$$\begin{aligned}\alpha_1 &= -4a_V, \\ \alpha_2 &= 12a_V - 0.65, \\ \beta &= -8a_V - 0.13\,, \end{aligned} \tag{18}$$

and this form has been used, for example, by KTeV [23] to fit their data with $a_V = -0.72 \pm 0.05 \pm 0.06$. In Eq. (18) β is no longer independent from $\alpha_{1,2}$; therefore it is clear that this *Ansatz* introduces model-dependent correlations between the B amplitude (the one responsible for a large CP-conserving $K_{\rm L} \to \pi^0 e^- e^-$), and the A amplitude which dominates the $K_{\rm L} \to \pi^0\gamma\gamma$ mode, but which does not contribute significantly to $K_{\rm L} \to \pi^0 e^+ e^-$.

2.1. Resonance models for α_1, α_2 and β

As mentioned before, the contribution of vector meson exchange, through diagrams such as that in figure 4 can be parameterized by the constant a_V. The constant a_V has been calculated in several models (there is no

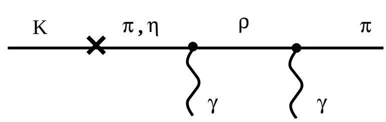

Fig. 4. One-loop diagrams responsible for $|\Delta S| = 1$ transitions in the Standard Model.

unique way to include vector mesons in the weak effective Lagrangian). The simplest ones are those that consider only pole diagrams such as figure 4. There also are possible direct weak terms, and a model to compute these direct counterterms is the "weak deformation model" of [19]. For this mode, the model predicts the direct weak counterterm contribution to a_V to be twice as large as that from the pole terms and to have the opposite sign. The net effect is thus to change the sign of the constant a_V calculated from pole diagrams alone. The chiral quark model is a different type of model that can also be parameterized by a_V alone [24]. The couplings that occur at order p^6 in a vector meson dominance model have been obtained in [19]. They are of the form

$$\mathcal{L}_V = \frac{G_8 \alpha_{\rm EM}}{4\pi} \frac{4a_V}{M_K^2} \left(\partial^\alpha K_{\rm L} \partial_\alpha \pi^0 F^{\mu\nu} F_{\mu\nu} + 2\partial_\alpha K_{\rm L} \partial^\beta \pi^0 F^{\alpha\mu} F_{\mu\beta} \right) \tag{19}$$

resulting in Eq. (18) (aside from small additional constants which appear in a particular regularization scheme for the loop amplitudes [18]). Although this pattern is a firm prediction of vector meson dominance models, a specific value for a_V is not. For example, in Ref. [19] the values $a_V = 0.32$ or $a_V = -0.32$ can be obtained depending on whether one uses the so called "weak deformation model" or not. This is just another way of saying that the concept of "vector meson dominance" is not uniquely defined for the weak interactions. In addition, phenomenological treatments of vector mesons such as those of Ref. [25] include effects from $\eta - \eta'$ mixing, which are formally of higher order, but which result in significantly different "vector meson" contributions to $K_{\rm L} \to \pi^0 \gamma\gamma$. It is worth mentioning that a quark model estimate of the parameters α_1, α_2 and β [24] yields the same pattern as in Eq. (18) with $a_V = (N_{\rm c}/27) g_{\rm A}^2 (M_K^2/m^2)$ in the notation of [24].

More recently, possible contributions from intermediate scalars and tensors have also been discussed. It is found that the tensor meson $f_2(1270)$, in particular, can contribute at a level comparable to that of vector mesons and yet produce a different pattern for the three constants [26, 27]. The effect of scalar resonances near 1 GeV turns out to be small [28]. The effect of a broad scalar resonance in the vicinity of 500 MeV would be important and several authors have considered this term. We prefer to include it in a different way, through a phenomenological pion re-scattering that comprises the additional p^6 contributions. The effect of resonances such as the $f_0(980)$ can be estimated as follows. First take the simplest form for the scalar–pion and scalar–photon interactions [29],

$$\mathcal{L}_S = g_\pi S \mathrm{Tr}\left(D^\mu \Sigma D_\mu \Sigma^\dagger \right) + \frac{\alpha_{\rm EM}}{4\pi} g_\gamma S F^{\mu\nu} F_{\mu\nu} \, . \tag{20}$$

The coupling g_π can be determined from the decay width of the scalar into two pions. Adding the charged and neutral modes we obtain

$$\Gamma(S \to \pi\pi) = \frac{3}{8\pi f_\pi^4} \sqrt{1 - 4r_{\pi s}^2} g_\pi^2 M_S^3 \left(1 - 2r_{\pi S}^2 + 4r_{\pi S}^4 \right) , \tag{21}$$

with $r_{\pi S} = M_\pi / M_S$. If we identify the scalar meson with the $f_0(980)$, and use the particle data book figures $B(f_0 \to \pi^+\pi^-) = 2/3$, $B(f_0 \to$

$\pi^0\pi^0) = 1/3$, [5] and the NOMAD result $\Gamma(f_0) = 35 \pm 12$ MeV [30] we find $g_\pi \sim \pm 5$ MeV (we cannot decide the sign ambiguity from the experimental rates).

The width for the scalar–meson decay into two photons allows us to determine g_γ. We find for the width

$$\Gamma(S \to \gamma\gamma) = \left(\frac{\alpha_{\rm EM}}{4\pi}\right)^2 \frac{g_\gamma^2 M_S^3}{4\pi}\,. \tag{22}$$

If again we identify the scalar with the $f_0(980)$ and use the particle data book value $\Gamma(f_0 \to \gamma\gamma) = 0.39^{+0.10}_{-0.13}\times 10^{-3}$ MeV [5], we find $g_\gamma \sim \pm 3.9\times 10^{-3}\,{\rm MeV}^{-1}$.

Collecting these results we finally obtain for the contribution of the scalar $f_0(980)$ to $K_{\rm L} \to \pi^0\gamma\gamma$ (see figure 5):

$$\alpha_1 = -\alpha_2 = 16 g_\pi g_\gamma \frac{M_K^2}{M_S^2} \sim \pm 0.08\,, \qquad \beta = 0\,. \tag{23}$$

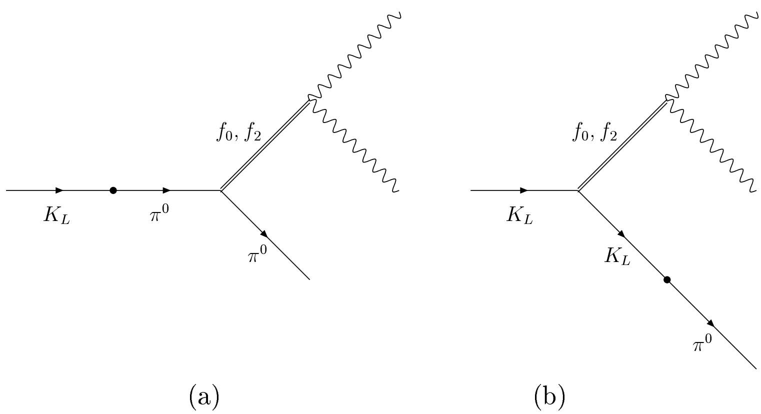

Fig. 5. Scalar– and tensor–meson resonance Feynman diagrams contributing to $K_{\rm L} \to \pi^0\gamma\gamma$. The dots in (a) and (b) represent flavor-changing mass-insertions in the incoming and outgoing particles, respectively [20, 21, 57].

In a similar manner we can determine the contribution from a tensor meson. A simple look at the low energy data for the reaction $\gamma\gamma \to \pi^0\pi^0$ [31] suffices to motivate the potential importance of the $f_2(1270)$ for our amplitudes through diagrams such as those in figure 5. Following Ref. [29] we write the lowest order couplings of a tensor meson $T_{\mu\nu}$ to pions and photons as

$$\mathcal{L}_T = h_\pi T^{\mu\nu}{\rm Tr}\left(D_\mu\Sigma D_\nu\Sigma^\dagger\right) + \frac{\alpha_{\rm EM}}{4\pi} h_\gamma T^{\mu\nu} F_{\mu\alpha} F_\nu^\alpha\,. \tag{24}$$

For the inclusive width of the tensor meson into two pions, and following Ref. [32] for the description of the spin 2 states, we obtain

$$\Gamma(T \to \pi\pi) = \frac{3h_\pi^2 M_T^3}{240\pi f_\pi^4}\left(1 - \frac{4m_\pi^2}{M_T^2}\right)^{5/2} . \tag{25}$$

For the decay width of the tensor meson into two photons we find

$$\Gamma(T \to \gamma\gamma) = \left(\frac{\alpha_{\rm EM}}{4\pi}\right)^2 \frac{h_\gamma^2 M_T^3}{80\pi} . \tag{26}$$

Identifying the tensor meson with the $f_2(1270)$ and using the particle data book values for mass and partial widths [5], we obtain $h_\pi \sim \pm 40$ MeV and $h_\gamma \sim \pm 0.03\ \text{MeV}^{-1}$.

The tensor (f_2) contribution to the parameters α_1, α_2 and β can be read from the interaction that results after the tensor meson has been integrated out

$$\mathcal{L}_T = \frac{G_8 \alpha_{\rm EM}}{4\pi}\frac{4h_\pi h_\gamma}{M_T^2}\left(\frac{2}{3}\partial^\alpha K_{\rm L}\partial_\alpha \pi^0 F^{\mu\nu}F_{\mu\nu} + 2\partial_\alpha K_{\rm L}\partial^\beta \pi^0 F^{\alpha\mu}F_{\mu\beta}\right). \tag{27}$$

The resulting contributions are:

$$\begin{aligned} \alpha_1 &= -\frac{4}{3}h_\pi h_\gamma \frac{M_K^2}{M_T^2} \sim \mp 0.25\,, \\ \alpha_2 &= \frac{28}{3}h_\pi h_\gamma \frac{M_K^2}{M_T^2} \sim \pm 1.7\,, \\ \beta &= -8h_\pi h_\gamma \frac{M_K^2}{M_T^2} \sim \mp 1.5\,. \end{aligned} \tag{28}$$

Table I summarizes the resonant contributions to the three parameters.

TABLE I

A comparison of parameters for $K_{\rm L} \to \pi^0\gamma\gamma$ for various resonant contributions.

	Vector ($a_V = \pm\ 0.32$)	Scalar	Tensor
α_1	$\mp$ 1.2	$\pm$ 0.08	$\mp$ 0.25
α_2	$\pm$ 3.6	$\mp$ 0.08	$\pm$ 1.7
β	$\mp$ 2.4	0	$\mp$ 1.5

2.2. The KTeV data

We now proceed to fit the KTeV results to our formulae. In figure 6 we reproduce the data from Ref. [23] as can be read from their published paper. We superimpose on the data the best fit we obtain in terms of the parameter a_V as a solid line. Our fit gives $a_V = -0.95$ with a $\chi^2/\text{d.o.f.} = 46/27$, which corresponds to

$$\begin{aligned}\alpha_1 &= 3.8\,,\\ \alpha_2 &= -12.0\,,\\ \beta &= 7.5\,.\end{aligned} \tag{29}$$

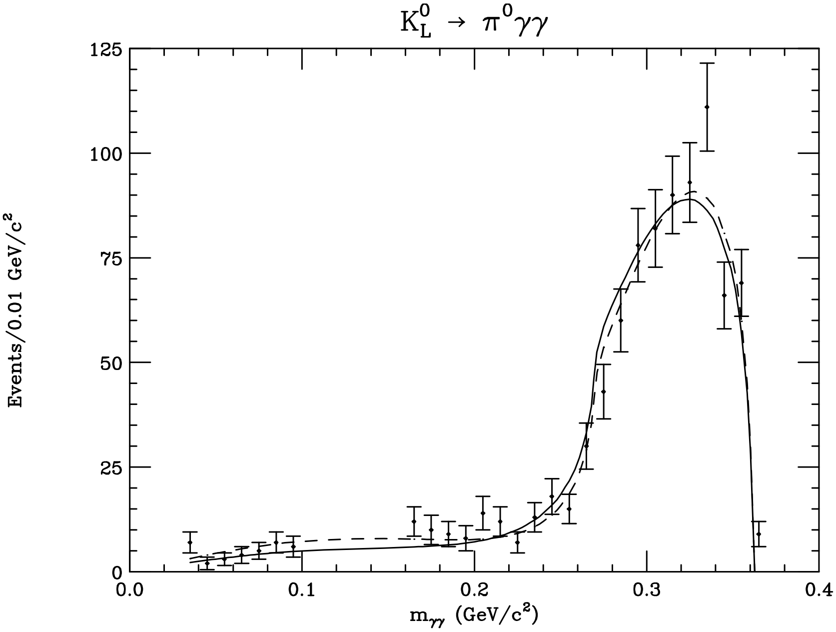

Fig. 6. Two different fits to the data from Ref. [23], as explained in the text. The solid line is a one-parameter fit corresponding to Eq. (29), the dashed line is the three-parameter fit shown in Eq. (30).

Notice that our value for a_V is not the same value quoted by Ref. [23] because we do not have access to the raw data and hence we have not taken into consideration any background or detector issues. Nevertheless, we feel that it is fair to compare this fit to our best three-parameter fit obtained in the same way. This one is presented in figure 6 as the dashed line, and corresponds to

$$\begin{aligned} \alpha_1 &= 0, \\ \alpha_2 &= 1.7\,, \\ \beta &= -5\,. \end{aligned} \tag{30}$$

For this fit we obtain a χ^2/d.o.f. = 37/25, slightly better than Eq. (29). Clearly it is up to the experiments to present a complete best fit to the data using the general form, Eqs. (12), (13), and taking into consideration all experimental issues. The KTeV fit was obviously performed using the shape of the distribution and ignoring the overall normalization. This is evident in that the theoretical rate corresponding to the best fit value of a_V disagrees with the measured rate. Much more instructive is a comparison with NA48 data that follows.

2.3. The NA48 result

The recently released NA48 data [33] is significantly different from the KTeV data and leads to different conclusions regarding the CP-conserving contribution to $K_{\rm L} \to \pi^0 e^+ e^-$ [34,35] as we will see below. Unlike KTeV, NA48 has presented their data in a form that allows us to directly compare our general fit to the usual VMD fit. This allows us to show that whereas it is possible to fit the decay distribution $d\Gamma/dm_{\gamma\gamma}$ equally well with the general and VMD approaches, only the former is capable of fitting simultaneously the decay distribution and the total decay rate.

2.4. Fitting the shape of the $d\Gamma/dm_{\gamma\gamma}$ distribution

NA48 has recently released their result for $K_{\rm L} \to \pi^0\gamma\gamma$ [33]. They analyze their data using Eq. (13) with the VMD assumption, and they find $a_V = -0.46$. For our fits we use the information in Table 2 of Ref. [33], which gives the number of unambiguous events, estimated background and acceptance for each 20 MeV bin in $m_{\gamma\gamma}$.

We begin our analysis with a fit to the shape of the $d\Gamma/dm_{\gamma\gamma}$ distribution, ignoring the measured branching ratio, to compare with the fit performed by NA48 (this is also what was done by KTeV). We calculate the number of events predicted in each bin as

$$N_i = N\left[\frac{1}{\Gamma_{K_{\rm L}}}\int_i dm_{\gamma\gamma}\left(\frac{d\Gamma}{dm_{\gamma\gamma}}\right)N(K_{\rm L})\right]\text{Acceptance}_i + \text{Background}_i\ , \tag{31}$$

where N is a normalization chosen to match the total number of events and $N(K_{\rm L}) = 23.9 \times 10^9$ is the number of decays in the fiducial volume. The arbitrary normalization allows us to fit the shape of the distribution while ignoring the overall rate.

We use data from 17 out of 20 bins presented in Table 2 of Ref. [33]. We exclude two bins in the $m_{\gamma\gamma}$ region near the π^0 mass which do not have any events due to kinematic cuts, and we also exclude the last bin with no events because it lies outside the physical region. We perform a least squares fit using Poisson statistics for the bins with small number of events following Ref. [36].

With this procedure, and the VMD *Ansatz*, we reproduce approximately the NA48 best fit. We obtain $a_V = -0.466$ with a $\chi^2/\text{d.o.f.} = 15.1/16$ [27]. We show this result in figure 7 where we superimpose our best three-parameter fit which has a $\chi^2/\text{d.o.f.} = 12.4/14$ [27]. The two fits are nearly identical as can be seen in the figure and they are indistinguishable statistically. Nevertheless, when they are both expressed in terms of the three general parameters one can see they correspond to very different solutions. For the general fit,

$$\alpha_1 = 4.51\,, \qquad \alpha_2 = -4.06\,, \qquad \beta = 0.93\,; \tag{32}$$

whereas for the VMD fit (in terms of a_V),

$$\alpha_1 = 1.86\,, \qquad \alpha_2 = -6.24\,, \qquad \beta = 3.60\,. \tag{33}$$

For the case of the three-parameter fit we find that α_1 and α_2 are correlated as was discussed in Ref. [26], so that there are many other fits with a χ^2 near the minimum for the same value of β.

As stated above, neither one of these fits reproduces the experimental rate, $B(K_{\rm L} \to \pi^0\gamma\gamma) = (1.36 \pm 0.03 \pm 0.03) \times 10^{-6}$ [33]. The theoretical branching ratio predicted for $a_V = -0.466$ (the NA48 value) is $B(K_{\rm L} \to \pi^0\gamma\gamma) = 1.1 \times 10^{-6}$, and the one predicted for the three parameters in Eq. (30) is $B(K_{\rm L} \to \pi^0\gamma\gamma) = 1.0 \times 10^{-6}$.

2.5. Simultaneous fit to the shape of the $d\Gamma/dm_{\gamma\gamma}$ distribution and to the decay rate

To obtain a fit that reproduces the observed branching ratio we proceed as in Eq. (31) but removing the arbitrary normalization,

$$N_i = \left[\frac{1}{\Gamma_{K_{\rm L}}}\int_i dm_{\gamma\gamma}\left(\frac{d\Gamma}{dm_{\gamma\gamma}}\right)N(K_{\rm L})\right]\text{Acceptance}_i + \text{Background}_i\,, \tag{34}$$

with the same notation of Eq. (31). We first attempt this fit with the VMD *Ansatz* and find that it is impossible to obtain a good fit. Our least squares fit using the VMD *Ansatz* occurs for $a_V = -0.64$ and has a $\chi^2/\text{d.o.f.} = 69.7/16$.

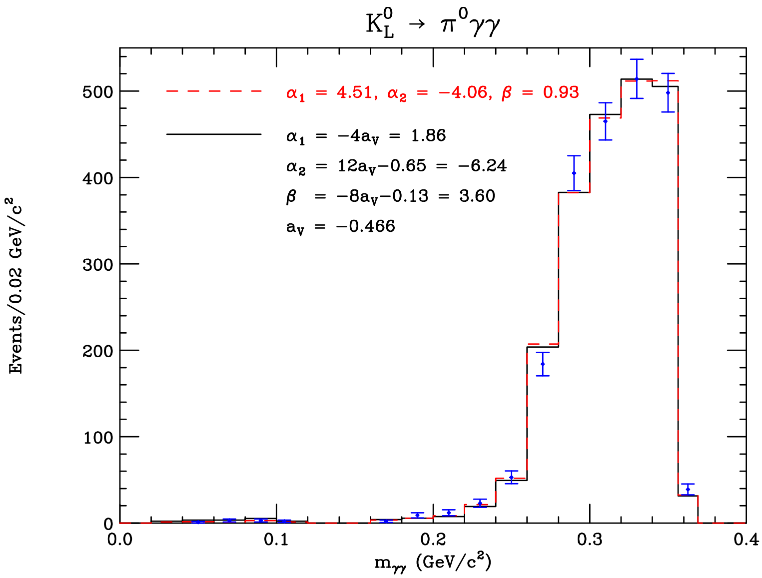

Fig. 7. Two different fits to the data from Ref. [33], as explained in the text. The solid line is a one-parameter fit corresponding to Eq. (33), the dashed line is the three-parameter fit shown in Eq. (32).

We show this result as the solid line in figure 8. The implied branching ratio is $B(K_{\rm L} \to \pi^0\gamma\gamma) = 1.27 \times 10^{-6}$ and $a_V = -0.64$ corresponds to

$$\alpha_1 = 2.56\ , \qquad \alpha_2 = -8.32\ , \qquad \beta = 4.99\ . \tag{35}$$

Our best three parameter fit, on the other hand, has a $\chi^2/\text{d.o.f.} = 15.8/14$ and is shown as the dashed line in figure 8. It implies a branching ratio $B(K_{\rm L} \to \pi^0\gamma\gamma) = 1.35 \times 10^{-6}$ in good agreement with the measured one. The parameters for this best fit are,

$$\alpha_1 = -2.59\ , \qquad \alpha_2 = -2.88\ , \qquad \beta = 0.57\,. \tag{36}$$

We conclude from figure 8 that the VMD *Ansatz* cannot reproduce the shape of the spectrum and the total decay rate simultaneously, but that the general formula, Eq. (13) does accommodate both. We hope KTeV implements the general analysis when they release their new result.

We now consider the dependence of our results on the parameter a_2 that appears in the B amplitude. This parameter is extracted from $K \to 3\pi$ decays and up to now we have used the value $a_2 = 6.5$ [18]. However, the value of this parameter has a large uncertainty, of order $\sim 35\,\%$. For example, from the recent analysis of Ref. [37] one extracts $a_2 = 6.8 \pm 2.4$.

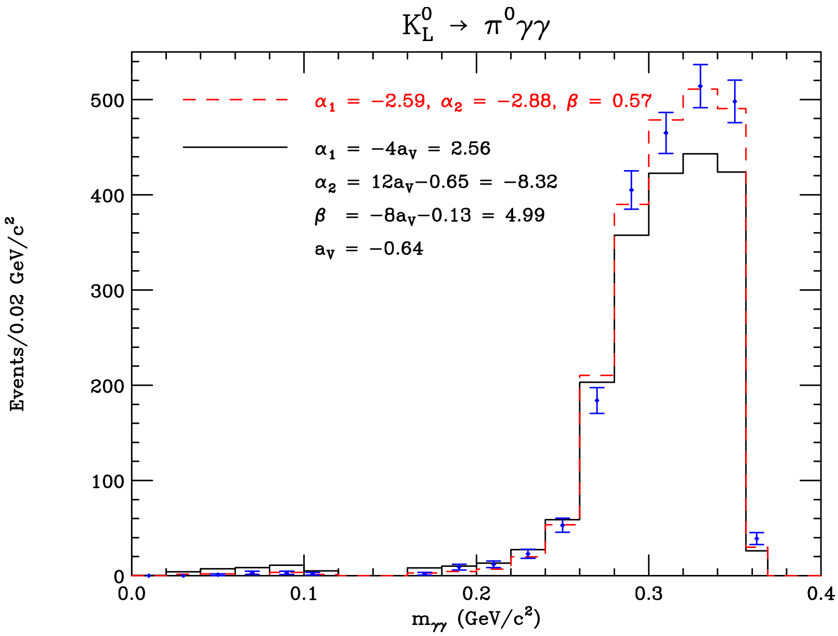

Fig. 8. A simultaneous fit to the shape of $d\Gamma/dm_{\gamma\gamma}$ and to the decay rate. The solid line is a one-parameter fit corresponding to Eq. (35), the dashed line is the three-parameter fit shown in Eq. (36).

The analytic form for the B amplitude in Eq. (13) clearly indicates that a_2 and β are correlated and this is confirmed by our numerical study. It is possible to obtain many equally good fits to the data with different values of a_2 and β. For example if we take the central value from Ref. [37] and 1-sigma deviations from it, we find good fits to the shape and spectrum with the values listed in Table II. This is not possible with the a_V parameterization, where we cannot find a good fit for any of these values of a_2.

TABLE II

Three-parameter best fits for three different values of a_2, corresponding to its central value from Ref. [37] and its 1-sigma deviations.

a_2	α_1	α_2	β	χ^2/d.o.f.
6.8	−2.82	−2.23	−0.03	16.2/14
4.4	−2.80	−1.31	−0.73	16.0/14
9.2	−2.72	−3.86	1.32	15.9/14

2.6. CP-conserving contribution to $K_\mathrm{L} \to \pi^0 e^+ e^-$

The estimate of this contribution starts with the absorptive contribution from the on-shell two-photon intermediate state to $K_\mathrm{L} \to \pi^0 e^+ e^-$, as depicted in figure 9.

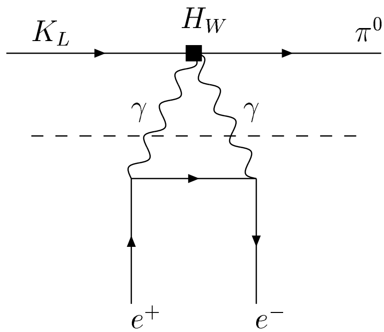

Fig. 9. Contribution from the on-shell two-photon intermediate state to $B_\mathrm{CP}(K_\mathrm{L} \to \pi^0 e^+ e^-)$.

The above contribution is not the full absorptive part since there is a further cut due to on-shell pions. Moreover, the full CP-conserving amplitude includes a contribution from the dispersive part of the amplitude, with off-shell photons (and pions). The general form of the amplitude is

$$\mathcal{M}_\mathrm{CP}(K_\mathrm{L} \to \pi^0 e^+ e^-) = G_8 \alpha_\mathrm{EM}^2 K p_K \cdot (k_{e^+} - k_{e^-})(p_K + p_\pi)^\mu \overline{u} \gamma_\mu v, \quad (37)$$

where K is the result of the loop calculation and the extra antisymmetry under $k_{e^+} \leftrightarrow k_{e^-}$ is a reflection of the properties under a CP transformation. Introducing a form factor to regularize the virtual photon couplings, an expression for K [35] is obtained:

$$K = \frac{B(x)}{16\pi^2 m_K^2} \left[\frac{2}{3} \log\left(\frac{m_\rho^2}{-s} \right) - \frac{1}{4} \log\left(\frac{-s}{m_e^2} \right) + \frac{7}{18} \right], \quad (38)$$

where $s = (k_{e^+} + k_{e^-})^2$. The log factor is of course expected, since the photon absorptive part comes from the expansion $\log(-s) = \log s + i\pi$. This representation of the amplitude leads to CP-conserving branching ratios as follows:

- Using the KTeV data:

$$B_\mathrm{CP}(K_\mathrm{L} \to \pi^0 e^+ e^-) = \begin{cases} 4.8 \times 10^{-12} & \text{VMD} \\ 7.3 \times 10^{-12} & \text{three-parameter fit.} \end{cases} \quad (39)$$

- Using the NA48 data, with only the results of the fit to the shape of the distribution, Eqs. (29) and (30),

$$B_{\rm CP}(K_{\rm L}\to\pi^0e^+e^-)=\begin{cases}4.5\times10^{-13} & \text{vector meson dominance}\\ 1.4\times10^{-13} & \text{three-parameter fit .}\end{cases} \tag{40}$$

- Using the results of the fits to both rate and spectrum measured by NA48, Eqs. (35) and (36), we find instead,

$$B_{\rm CP}(K_{\rm L}\to\pi^0e^+e^-)=\begin{cases}14.6\times10^{-13} & \text{vector meson dominance}\\ 2.7\times10^{-13} & \text{three-parameter fit .}\end{cases} \tag{41}$$

Notice that the numbers obtained from NA48 data are an order of magnitude smaller than what is obtained using the KTeV data. We can see from figure 10 why the NA48 result [33] implies a much smaller $B_{\rm CPC}(K_{\rm L}\to\pi^0e^+e^-)$ than the KTeV result [23] ($\beta=-5$ for the three-parameter fit or $\beta=7.5$ for the a_V fit). These two points are shown as the two internal dotted lines in figure 10. It is clear from this figure that the NA48 results correspond to a $K_{\rm L}\to\pi^0\gamma\gamma$ that produces a minimal CP-conserving contribution in $K_{\rm L}\to\pi^0e^+e^-$, *i.e.* it indicates that the two photons have a negligible D-wave component. The VMD result in Eq. (40) is consistent with the result reported by NA48. The latter is based on an analysis of the low $m_{\gamma\gamma}$ region only and yields $B_{\rm CPC}(K_{\rm L}\to\pi^0e^+e^-)=(4.7^{+2.2}_{-1.8})\times10^{-13}$ [33]. The NA48 result is obtained from data with $m_{\gamma\gamma}$ below 110 MeV and is therefore model independent because in that region the B amplitude dominates and the correlation with the A amplitude implied by the VMD *Ansatz* disappears.

The two points from the complete fit (rate and spectrum) are shown as the external dotted lines in figure 10. Not surprisingly, the general three-parameter fit continues to agree with the model independent NA48 limit as it gives a good fit to both the rate and spectrum. On the other hand, the fit in terms of a_V alone does not reproduce the data very well and we can dismiss its implication of a larger $B_{\rm CP}(K_{\rm L}\to\pi^0e^+e^-)$.

In figure 10 we see why there are two different solutions for β that result in the same $B_{\rm CPC}(K_{\rm L}\to\pi^0e^+e^-)$. This CP-conserving component depends quadratically on the $B(z)$ amplitude of $K_{\rm L}\to\pi^0\gamma\gamma$, and therefore there are two values of β for any given $B_{\rm CPC}(K_{\rm L}\to\pi^0e^+e^-)$. They correspond to constructive and destructive interference between the term with a_2 and β in Eq. (13).

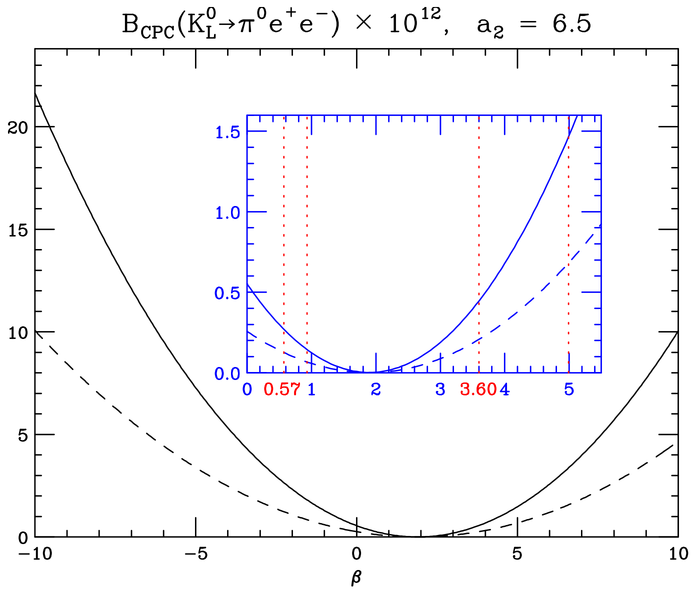

Fig. 10. CP-conserving contribution to $K_{\rm L} \to \pi^0 e^+ e^-$ as a function of β with $a_2 = 6.5$ [18]. The dashed line shows the absorptive contribution and the solid line the model of Ref. [35]. The enlargement shows the results for the branching ratio *vs.* the four values of $\beta = 0.57$, 0.93, 3.60 and 4.99 from the three- and one-parameter fits discussed in the text. These are marked by vertical dotted lines.

2.7. Conclusions on $K_{\rm L} \to \pi^0 \gamma\gamma$

The NA48 data for the reaction $K_{\rm L} \to \pi^0 \gamma\gamma$ can be accommodated nicely by the theoretical expression based on chiral perturbation theory at order p^6. With this expression it is possible to describe simultaneously the total rate and the shape of the spectrum, which is not possible with chiral perturbation theory at order p^4 [16]. The commonly used VMD *Ansatz* fails in this case, and that it is impossible to fit both the rate and the shape of the spectrum if this *Ansatz* is adopted, this is true for both the KTeV and NA48 data sets.

The new results from NA48 indicate a very small D-wave component for the photon pair and this leads to a prediction of a negligible CP-conserving background to $K_{\rm L} \to \pi^0 e^+ e^-$. We have shown that this result is not an artifact of the VMD *Ansatz* and that it holds in the general parameterization. This result is at odds with the earlier KTeV data and we must wait for the new KTeV results to see how this discrepancy is resolved.

3. Hyperon decay

I discuss CP violation in $\Lambda \to p\pi^-$ contrasting the standard model expectations with upper bounds that can be saturated in new physics scenarios. I review recent progress in the theoretical estimates.

3.1. Introduction

In non-leptonic hyperon decays such as $\Lambda \to p\pi^-$ it is possible to search for CP-violation by comparing the angular distribution with the corresponding anti-hyperon decay [38]. The Fermilab experiment HyperCP is currently analyzing data searching for CP-violation in such a decay.

The reaction of interest for HyperCP is the decay of a polarized Λ, with known polarization $\boldsymbol{w}$, into a proton (whose polarization is not measured) and a π^- with momentum $\boldsymbol{q}$. The interesting observable is a correlation in the decay distribution of the form

$$\frac{\mathrm{d}\Gamma}{\mathrm{d}\Omega} \sim 1 + \alpha\, \boldsymbol{w} \cdot \boldsymbol{q} \ . \tag{42}$$

The branching ratio for this mode is 63.9% and the parameter α has been measured to be $\alpha_\Lambda = 0.64$ [5]. The CP-violation in question involves a comparison of the parameter α with the corresponding parameter $\bar{\alpha}$ from the reaction $\bar{\Lambda} \to \bar{p}\pi^+$.

To obtain polarized Λ's with known polarization, it is necessary to study the double decay chain $\Xi^- \to \Lambda\pi^- \to p\pi^-\pi^-$ [39,40]. This eventually leads to the experimental observable being sensitive to the *sum* of CP-violation in the Ξ decay and CP-violation in the Λ decay.

It is standard to write the amplitudes in terms of their isospin components in the form

$$\begin{aligned} S &= S_1 e^{i\delta_1^S} + S_3 e^{i\delta_3^S} \ , \\ P &= P_1 e^{i\delta_1^P} + P_3 e^{i\delta_3^P} \ . \end{aligned} \tag{43}$$

A $\Delta I = 1/2$ rule is observed experimentally, $S_3/S_1 \approx 0.026$ and $P_3/P_1 = 0.03 \pm 0.03$ [41]. The strong πN scattering phases have been measured for the $I = 1/2$ channel, $\delta_1^S \sim 6^\circ$ and $\delta_1^P \sim -1^\circ$ [42]. The $I = 3/2$ scattering phases have been measured with large errors but are not needed here.

To discuss CP violation, we allow the amplitudes in Eq. (43) to have a CP-violating weak phase, $S_i \to S_i \exp(i\phi_i^S)$ and $P_i \to P_i \exp(i\phi_i^P)$ and compare the pair of CP conjugate reactions. CP symmetry predicts that $\Gamma = \bar{\Gamma}$ and that $\bar{\alpha} = -\alpha$. One therefore defines the CP-odd observables

$$\begin{aligned} \Delta &\equiv \frac{\Gamma - \bar{\Gamma}}{\Gamma + \bar{\Gamma}} \sim \sqrt{2}\frac{S_3}{S_1}\sin(\delta_3^S - \delta_1^S)\sin(\phi_3^S - \phi_1^S)\,, \\ A(\Lambda^0_-) &\equiv \frac{\alpha + \bar{\alpha}}{\alpha - \bar{\alpha}} \sim -\sin(\delta_1^P - \delta_1^S)\sin(\phi_1^P - \phi_1^S) \sim 0.12\sin(\phi_1^P - \phi_1^S)\,. \end{aligned} \tag{44}$$

The partial rate asymmetry is very small, being suppressed by three small factors, S_3/S_1, strong phases, and weak phases. It represents an interference between amplitudes with $\Delta I = 1/2$ and $\Delta I = 3/2$. The asymmetry $A(\Lambda^0_-)$, on the other hand, is not suppressed by the $\Delta I = 1/2$ rule, as it originates in an interference of S and P-waves within the $\Delta I = 1/2$ transition. For this reason, the observable $A(\Lambda^0_-)$ is *qualitatively* different from ε'/ε.

The experimental observable is [39, 40],

$$A_{\Xi\Lambda} \approx A_\Lambda + A_\Xi\,, \tag{45}$$

and the current limit from E756 is $A_{\Xi\Lambda} = 0.012 \pm 0.014$ [39], and the expected sensitivity of HyperCP is 10^{-4} [40]. Previous estimates for $A_{\Xi\Lambda}$ indicated that it occurs at the few times 10^{-5} level within the standard model [43–45] and that it can be as large as 10^{-3} beyond the standard model [43,46–48]. The larger asymmetries occur in models with an enhanced gluon dipole operator that is parity-even and thus does not contribute to ε'. The 10^{-3} upper bound corresponds to the phenomenological constraint from new contributions to the ε parameter in kaon decay. This illustrates the relevance of the HyperCP measurement which complements the ε' experiments in the study of CP-violation in $\Delta S = 1$ transitions.

The strong πN scattering phases needed have been measured to be $\delta_S^\Lambda \sim 6^\circ$ and $\delta_P^\Lambda \sim -1^\circ$ with errors of about 1° [42]. In contrast, the strong $\Lambda\pi$ scattering phases have not been measured. Modern calculations based on chiral perturbation theory indicate that these phases are small, with $|\delta_S^\Xi|$ at most 7° [49–54]. For our numerical results, we will allow the $\Lambda\pi$ phases to vary within the range obtained at next-to-leading order in heavy-baryon chiral perturbation theory [52],

$$-3.0^\circ \le \delta_S^\Xi \le +0.4^\circ\,, \qquad -3.5^\circ \le \delta_P^\Xi \le -1.2^\circ\,. \tag{46}$$

Eventually these phases can be extracted directly from the measurement of the decay distribution in $\Xi \to \Lambda\pi$ [40]. I now summarize the efforts to determine the weak phases.

3.2. Chiral perturbation theory

The chiral Lagrangian that describes the interactions of the lowest-lying mesons and baryons is written down in terms of the lightest meson-octet, baryon-octet, and baryon-decuplet fields [55–58]. I will illustrate the terms involving octet fields only and refer you to the literature for incorporating the decuplet. The meson and baryon octets are collected into 3×3 matrices φ and B. The octet mesons enter as discussed before.

In the heavy-baryon formalism [58, 59], the baryons in the chiral Lagrangian are described by velocity-dependent fields, B_v. For the strong interactions, the leading-order Lagrangian is given by [58–60]

$$\mathcal{L}_{\rm s}^{(1)} = {\rm Tr}(\bar{B}_v\, {\rm i}v\cdot\mathcal{D}B_v) + 2D{\rm Tr}\left(\bar{B}_v S_v^\mu \left\{\mathcal{A}_\mu, B_v\right\}\right) + 2F{\rm Tr}\left(\bar{B}_v S_v^\mu \left[\mathcal{A}_\mu, B_v\right]\right)\,, \tag{47}$$

where S_v is the spin operator, and

$$\mathcal{A}_\mu = \tfrac{\rm i}{2}\left(\xi\,\partial_\mu\xi^\dagger - \xi^\dagger\,\partial_\mu\xi\right) = \frac{\partial_\mu\varphi}{2f} \;+\; \mathcal{O}(\varphi^3)\,, \tag{48}$$

with further details given in Ref. [61]. In this Lagrangian, D, F and other constants associated with the decuplet are free parameters which can be determined from hyperon semi-leptonic decays. Fitting tree-level formulas, one extracts [58, 59]

$$D = 0.80\,, \qquad\qquad F = 0.50\,. \tag{49}$$

The nonrelativistic quark model yields relations [60] between these parameters.

At next-to-leading order, the strong Lagrangian contains a greater number of terms [62]. The ones of interest here are those that explicitly break chiral symmetry, containing one power of the quark-mass matrix $M = {\rm diag}(0,0,m_s)$. For our calculation of the factorization of the penguin operator we will need these terms in the form,

$$\begin{aligned}\mathcal{L}_{\rm s}^{(2)} \;&=\; \tfrac{1}{4}f^2{\rm Tr}(\chi_+) + \frac{b_D}{2B_0}{\rm Tr}(\bar{B}_v\left\{\chi_+, B_v\right\}) \\ &+\; \frac{b_F}{2B_0}{\rm Tr}(\bar{B}_v\left[\chi_+, B_v\right]) + \frac{b_0}{2B_0}{\rm Tr}(\chi_+){\rm Tr}(\bar{B}_v B_v)\,,\end{aligned} \tag{50}$$

where we have used the notation $\chi_+ = \xi^\dagger\chi\xi^\dagger + \xi\chi^\dagger\xi$ to introduce coupling to external (pseudo)scalar sources $\chi = s + ip$ such that in the absence of the external sources this term reduces to the mass matrix $\chi = 2B_0 M$. As will be discussed in the next section, we also need from the meson sector the next-to-leading-order Lagrangian

$$\mathcal{L}_{\rm s}^{(4)} \;=\; L_5{\rm Tr}(\partial^\mu\Sigma^\dagger\partial_\mu\Sigma\,\xi^\dagger\chi_+\xi) \;+\; \cdots\,, \tag{51}$$

where only the relevant term is explicitly shown. In these Lagrangians, B_0, $b_{D,F,0}$, c, c_0, and L_5 are free parameters to be extracted from data.

As in the meson sector, the weak interactions responsible for hyperon non-leptonic decays are described by a $|\Delta S| = 1$ Hamiltonian that transforms as $(8_{\rm L}, 1_{\rm R}) \oplus (27_{\rm L}, 1_{\rm R})$ under $\mathrm{SU}(3)_{\rm L} \times \mathrm{SU}(3)_{\rm R}$ rotations. It is also known from experiment that the octet term dominates the 27-plet term, as indicated by the fact that the $|\Delta I| = 1/2$ components of the decay amplitudes are larger than the $|\Delta I| = 3/2$ components by about twenty times [41, 61]. We shall, therefore, assume in what follows that the decays are completely characterized by the $(8_{\rm L}, 1_{\rm R})$, $|\Delta I| = 1/2$ interactions. The leading-order chiral Lagrangian for such interactions is [55, 63]

$$\mathcal{L}_{\rm w} = h_D \mathrm{Tr}\left(\bar{B}_v \left\{\xi^\dagger h \xi \,,\, B_v\right\}\right) + h_F \mathrm{Tr}\left(\bar{B}_v \left[\xi^\dagger h \xi \,,\, B_v\right]\right) \,, \tag{52}$$

where h is a $3{\times}3$ matrix with elements $h_{ij} = \delta_{i2}\delta_{3j}$, and the parameters $h_{D,F}$ contain the weak phases.

The Lagrangian Eq. (52) is thus the leading-order (in χPT) realization of the effective $|\Delta S| = 1$ Hamiltonian in the standard model,

$$\mathcal{H}_{\rm w} = \frac{G_{\rm F}}{\sqrt{2}} V_{ud}^* V_{us} \sum_{i=1}^{10} C_i \, Q_i \; + \; \mathrm{H.c} \,, \tag{53}$$

where $G_{\rm F}$ is the Fermi coupling constant, V_{kl} are elements of the Cabibbo–Kobayashi–Maskawa (CKM) matrix [2],

$$C_i \;\equiv\; z_i + \tau y_i \;\equiv\; z_i \,-\, \frac{V_{td}^* V_{ts}}{V_{ud}^* V_{us}} \, y_i \tag{54}$$

are the Wilson coefficients, and Q_i are four-quark operators whose expressions can be found in Ref. [7]. Writing the V_{kl} in the Wolfenstein parameterization [3] we have

$$V_{ud}^* V_{us} = \lambda \,, \qquad\qquad V_{td}^* V_{ts} = -\lambda^5 A^2 \,(1 - \rho + i\eta) \tag{55}$$

at lowest order in λ. For our numerical estimates, we will employ [64]

$$\lambda = 0.2219 \,, \qquad A = 0.832 \,, \qquad \eta = 0.339 \;. \tag{56}$$

We now have all the ingredients necessary to calculate the weak decay amplitudes in terms of the parameters $h_{D,F}$ and γ_8 (only the first two are needed at leading order and γ_8 is related to g_8 discussed earlier). The amplitude for the weak decay of a spin-$\frac{1}{2}$ baryon B into another spin-$\frac{1}{2}$ baryon B' and a pseudoscalar meson φ has the general form [63]

$$i\mathcal{M}_{B\to B'\phi} = -i\langle B'\phi|\mathcal{L}_{\rm w+s}|B\rangle = \bar{u}_{B'} \left(\mathcal{A}^{(S)} + 2S_v{\cdot}p_\phi \, \mathcal{A}^{(P)}\right) u_B \,, \tag{57}$$

where the superscripts refer to the S- and P-wave components of the amplitude. We further follow the convention [63],

$$a^{(S,P)}_{BB'\phi} \equiv \sqrt{2}\, f\, \mathcal{A}^{(S,P)}_{B\to B'\phi} \tag{58}$$

to express our results. With the Lagrangians given above, one can derive the amplitudes at leading order, represented by the diagrams in figure 11. The figure indicates that the S-wave is directly obtained from a weak vertex from Eq. (52). The leading contribution to the P-wave arises from baryon-pole diagrams which involve a weak vertex from Eq. (52), a strong vertex from Eq. (47), and a mass difference (for the baryon propagator) from Eq. (50). The leading order results are [55, 57, 63],

$$\begin{aligned}
a^{(S)}_{\Sigma^+ n\pi^+} &= 0\,, \qquad\qquad a^{(S)}_{\Sigma^- n\pi^-} = -h_D + h_F\,, \\
a^{(S)}_{\Lambda p\pi^-} &= \tfrac{1}{\sqrt{6}}(h_D + 3h_F)\,, \quad a^{(S)}_{\Xi^-\Lambda\pi^-} = \tfrac{1}{\sqrt{6}}(h_D - 3h_F)\,, \\
a^{(P)}_{\Sigma^+ n\pi^+} &= \frac{-D\,(h_D - h_F)}{m_\Sigma - m_N} - \frac{\frac{1}{3}D\,(h_D + 3h_F)}{m_\Lambda - m_N}\,, \\
a^{(P)}_{\Sigma^- n\pi^-} &= \frac{-F\,(h_D - h_F)}{m_\Sigma - m_N} - \frac{\frac{1}{3}D\,(h_D + 3h_F)}{m_\Lambda - m_N}\,, \\
a^{(P)}_{\Lambda p\pi^-} &= \frac{2D\,(h_D - h_F)}{\sqrt{6}\,(m_\Sigma - m_N)} + \frac{(D+F)\,(h_D + 3h_F)}{\sqrt{6}\,(m_\Lambda - m_N)}\,, \\
a^{(P)}_{\Xi^-\Lambda\pi^-} &= \frac{-2D\,(h_D + h_F)}{\sqrt{6}\,(m_\Xi - m_\Sigma)} - \frac{(D-F)\,(h_D - 3h_F)}{\sqrt{6}\,(m_\Xi - m_\Lambda)}\,.
\end{aligned} \tag{59}$$

The leading nonanalytic contributions to the amplitudes have been calculated by various authors [55,63,65,66]. We will adopt the results of Ref. [66] for the numerical estimate of our uncertainty.

Once we specify the value of the weak couplings $h_{D,F}$ the expressions in Eq. (59) determine the leading order amplitudes. It is well known that this representation does not provide a good fit to the measured P-wave amplitudes, and that higher order terms are important [55, 57, 63, 65–67]. The procedure that we adopt to estimate the weak phases is to obtain the real part of the amplitudes from experiment (assuming no CP-violation), and to use Eq. (59) to estimate the imaginary parts. The dominant CP-violating phases in the $|\Delta I| = 1/2$ sector of the $|\Delta S| = 1$ weak interaction occur in the Wilson coefficient C_6 associated with the penguin operator Q_6. Our strategy will be to calculate within a model the imaginary part of the couplings $h_{D,F,C}$ and γ_8 induced by Q_6. As a numerical result we propose a central value from leading order χPT (Eq. (59)), and an estimate of the error from the non-analytic corrections obtained with the expressions in Ref. [66].

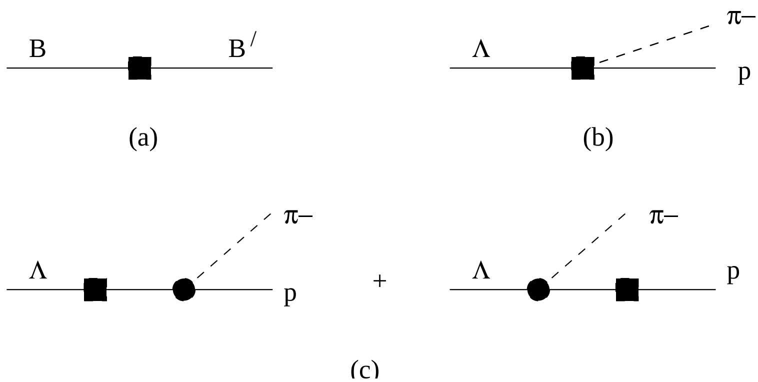

Fig. 11. (a) $B \to B'$ transition due to Q_6, solid square. (b) S-wave obtained from (a) via a soft-pion theorem. (c) P-wave obtained from (a) with strong pion emission (solid circle).

3.3. Estimate of counterterms

Our goal is to match the dominant $|\Delta I| = 1/2$ CP-violating term from the standard model effective weak Hamiltonian in Eq. (53) to the weak chiral Lagrangian in Eq. (52). That is, to compute the imaginary part of the parameters h_D, h_F and γ_8 that is induced by $\mathrm{Im}\, C_6 Q_6$ in Eq. (53).

To do this we will include both factorizable contributions that arise from regarding the operator Q_6 as the product of two (pseudo)scalar densities, and direct (non-factorizable) contributions calculated in the MIT bag model.

The non-factorizable contributions are easily obtained from the observation that the weak chiral Lagrangian of Eq. (52) is responsible for non-diagonal "weak mass terms" such as

$$\begin{aligned} \langle n|(\mathcal{H}_\mathrm{w})_8|\varLambda\rangle &= \frac{h_D + 3h_F}{\sqrt{6}}\, \bar{u}_n u_\varLambda \,, \\ \langle \varLambda|(\mathcal{H}_\mathrm{w})_8|\varXi^0\rangle &= \frac{h_D - 3h_F}{\sqrt{6}}\, \bar{u}_\varLambda u_\varXi \,, \\ \langle \varXi^{*-}|(\mathcal{H}_\mathrm{w})_8|\varOmega^-\rangle &= -\frac{h_C}{\sqrt{3}}\, \bar{u}_{\varXi^*} \cdot u_\varOmega \,, \end{aligned} \tag{60}$$

where the subscript 8 denotes the component of $\mathcal{H}_\mathrm{w}$ that transforms as $(8_\mathrm{L}, 1_\mathrm{R})$. These terms can be computed directly from the short-distance Hamiltonian in Eq. (53) by calculating the baryon–baryon matrix elements of the four-quark operators in the MIT bag model [68],

$$\mathrm{Im}\, h_D = 0.028\ y_6 \,, \qquad \mathrm{Im}\, h_F = 0.25\ y_6 \,, \tag{61}$$

The units are $(\sqrt{2} f_\pi G_{\rm F} m_\pi^2 \lambda^4 A^2 \eta)$, chosen to separate both the conventional normalization for the hyperon decay amplitudes as in Eq. (58) and the relevant combination of CKM parameters that occurs in the observable A.

To obtain the factorizable contributions to the imaginary part of the parameters $h_{D,F,C}$ we follow the procedure used in kaon physics for γ_8 [69]. We start from the observation that the quark-mass terms in the QCD Lagrangian can be written as

$$\mathcal{L}_m = -\frac{1}{2B_0}\left(\bar{q}_{\rm L}\,\chi\, q_{\rm R} + \bar{q}_{\rm R}\,\chi^\dagger\, q_{\rm L}\right)\,, \tag{62}$$

where $q_{\rm L} = \frac{1}{2}(1-\gamma_5)q$ and $q_{\rm R} = \frac{1}{2}(1+\gamma_5)q$, with $q = (u\ \ d\ \ s)^{\rm T}$. It follows that

$$\begin{aligned} -\bar{q}_{l{\rm L}}\, q_{k{\rm R}} &= 2B_0\,\frac{\delta\mathcal{L}_m}{\delta\chi_{lk}}\,, \\ -\bar{q}_{l{\rm R}}\, q_{k{\rm L}} &= 2B_0\,\frac{\delta\mathcal{L}_m}{\delta\chi^\dagger_{lk}}\,. \end{aligned} \tag{63}$$

The weak Lagrangian corresponding to a factorized Q_6 is then given by Eq. (52) with

$$h_D = \frac{G_{\rm F}\,\lambda}{\sqrt{2}}\,8\,C_6\,f^2 B_0\,b_D\,, \qquad h_F = \frac{G_{\rm F}\,\lambda}{\sqrt{2}}\,8\,C_6\,f^2 B_0\,b_F\,. \tag{64}$$

The values of b_D, b_F can be found by fitting the mass formulas derived from the Lagrangian in Eq. (50), with $\chi = 2B_0 M$, to the measured masses of the octet and decuplet baryons. Thus one finds

$$b_D\, m_s = 0.0301\ \text{GeV}\,, \qquad b_F\, m_s = -0.0948\ \text{GeV}\,, \tag{65}$$

for $m_u = m_d = 0$. In this limit, the Lagrangian in Eq. (50) also gives $m_K^2 = B_0\, m_s$. Using $m_s = \bar{m}_s(\mu = m_{\rm c}) = 170\,\text{MeV}$ from Ref. [7], one then has

$$b_D = 0.177\,, \qquad b_F = -0.558\,, \qquad c = 1.30\,, \qquad B_0 = 1.45\,\text{GeV}\,. \tag{66}$$

Correspondingly we use for our numerical estimates

$$B_0(\mu) = \left[\frac{m_K^2}{m_s(\mu) + m_d(\mu)}\right] \sim 1.38\ \text{GeV}\ .$$

3.4. Numerical results

If Eq. (59) provided a good fit to the hyperon decay amplitudes, it would be straightforward to calculate the weak phases of Eq. (44). We would simply divide the imaginary parts of the amplitudes by the real part of the amplitudes obtained from a matching of the parameters $h_{D,F}$ to the short distance Hamiltonian. However, as we mentioned before, leading-order chiral perturbation theory fails to reproduce simultaneously the S- and P-wave amplitudes. Consequently we are forced to employ the real part of the amplitudes that are extracted from experiment under the assumption of no CP violation.

We assume that the real part of the weak decay amplitudes originates predominantly in the tree-level operators $Q_{1,2}$, and that the imaginary part of the amplitudes is primarily due to the $\mathrm{Im}\, C_6 Q_6$ term in the weak Hamiltonian. This is true both in the bag model and in the vacuum saturation model of Ref. [44]. With these assumptions we calculate a central value for the imaginary part of the weak decay amplitudes using Eq. (59) with values for $\mathrm{Im}\, h_{D,F}$ obtained in the previous section by adding the factorizable and non-factorizable contributions. We estimate the uncertainty in this prediction by computing the leading non-analytic corrections with our values for $\mathrm{Im}\ h_{D,F}$.

For the numerical results below, we use the leading-order (in QCD) Wilson coefficients at $\mu = m_{\rm c} = 1.3\,\mathrm{GeV}$ listed in Table XIX of Ref. [7]. In particular,

$$y_6 = -0.096\,, \tag{67}$$

corresponding to $\Lambda_{\overline{\rm MS}}^{(4)} = 325\,\mathrm{MeV}$.

Numerically we find uncertainties in ϕ_S and ϕ_P of order 100% and 50%, respectively, for both decays. We present our predictions for these phases and also the resulting phase differences in Table III [68]. The errors for the differences have been obtained by adding the individual errors. We have also collected strong-phase differences in this table. Combining these results we

TABLE III

Weak phases in units of $\eta\lambda^5 A^2$, and strong-phase differences, $\delta_S - \delta_P$.

Decay mode	ϕ_S	ϕ_P	$\phi_S - \phi_P$	$\delta_S - \delta_P$
$\Lambda \to p\pi^-$	1.0 ± 1.0	1.2 ± 0.6	-0.2 ± 1.6	$7^\circ \pm 2^\circ$
$\Xi^- \to \Lambda\pi^-$	0.9 ± 0.9	-0.6 ± 0.3	1.5 ± 1.2	$1.1^\circ \pm 2.8^\circ$

finally obtain

$$\begin{aligned} A(\Lambda^0_-) &= A_\Lambda = (0.03 \pm 0.25)\ A^2\lambda^5\eta\,, \\ A(\Xi^-_-) &= A_\Xi = (-0.05 \pm 0.13)\ A^2\lambda^5\eta\,, \end{aligned} \tag{68}$$

leading to

$$A_{\Xi\Lambda} = A_\Lambda + A_\Xi = (-0.02 \pm 0.38)\ A^2\lambda^5\eta\ . \tag{69}$$

With the CKM parameter values given in Eq. (56), we have $A^2\lambda^5\eta \simeq 1.26\times 10^{-4}$ and, therefore,

$$-3\times 10^{-5} \ \leq\ A_\Lambda \leq 4\times 10^{-5}\,, \qquad -2\times 10^{-5} \leq A_\Xi \leq 1\times 10^{-5}\,, \tag{70}$$

$$-5\times 10^{-5} \ \leq\ A_{\Xi\Lambda} \leq 5\times 10^{-5}\,. \tag{71}$$

3.5. Beyond the Standard Model

There have been several estimates of $A(\Lambda^0_-)$ beyond the standard model. For the most part these studies discuss specific models, concentrating on one or a few operators and normalizing the strength of CP violation by fitting ε. Some of these results (which have not been updated to incorporate current constraints on model parameters) are:

$$A(\Lambda^0_-) = \begin{cases} -2\times 10^{-5} & \text{SM [43]} \\ -2\times 10^{-5} & \text{3 Higgs [43]} \\ 0 & \text{Superweak} \\ 6\times 10^{-4} & \text{LR [47]} \end{cases} \tag{72}$$

Perhaps a more interesting question is whether it is possible to have large CP violation in hyperon decays in view of what is known about ε and ε'. This question has been addressed in a model independent way by considering all the CP-violating operators that can be constructed at dimension 6 that are compatible with the symmetries of the standard model [46]. With this general formalism one can compute the contributions of each new CP-violating phase to $\varepsilon, \varepsilon'$, and $A(\Lambda^0_-)$. Of course, there is the caveat that the hadronic matrix elements cannot be computed reliably. Nevertheless, one finds in general, that parity even operators generate a weak phase ϕ_1^P and do not contribute to ε'. Their strength can be bound from the long distance contributions to ε that they induce. Similarly, the parity-odd operators generate a weak phase ϕ_1^S and contribute to ε' (but not to ε).

The constraints from ε' turn out to be much more stringent than those from ε, and, therefore, the only natural way (without invoking fine cancellations between different operators) to obtain a large $A(\Lambda^0_-)$ given what we know about ε' is with new CP-odd, P-even interactions. Within the model independent analysis, one can identify a few new operators with the required properties, that can lead to [46],

$$A(\Lambda^0_-) \sim 5 \times 10^{-4} \quad \mathrm{P-even, CP-odd}\,. \tag{73}$$

This possibility has been revisited recently, motivated in part by the observation of ε'. The average value $\varepsilon'/\varepsilon = (21.2 \pm 4.6) \times 10^{-4}$ [70] appears to be larger than the standard model central prediction with simplistic models for the hadronic matrix elements. This has motivated searches for new sources of CP violation that can give large contributions to ε', in particular, within supersymmetric theories. One such scenario generates a large ε' through an enhanced gluonic dipole operator [71]. The effective Hamiltonian is of the form

$$\begin{aligned} H_{\mathrm{eff}} &= (\delta^d_{12})_{\mathrm{LR}} C_g \bar{d}\sigma_{\mu\nu} t^a (1+\gamma_5) s G^{a\mu\nu} \\ &+ (\delta^d_{12})_{\mathrm{RL}} C_g \bar{d}\sigma_{\mu\nu} t^a (1-\gamma_5) s G^{a\mu\nu}\,. \end{aligned} \tag{74}$$

The quantity C_g is a known loop factor, and the $(\delta^d_{12})_{\mathrm{LR,RL}}$ originate in the supersymmetric theory [72]. Depending on the correlation between the value of $(\delta^d_{12})_{\mathrm{LR}}$ and $(\delta^d_{12})_{\mathrm{RL}}$ one gets different scenarios for ε' and $A(\Lambda^0_-)$ as shown in figure 2 [48]. For example, if only $(\delta^d_{12})_{\mathrm{LR}}$ is non-zero, there can be

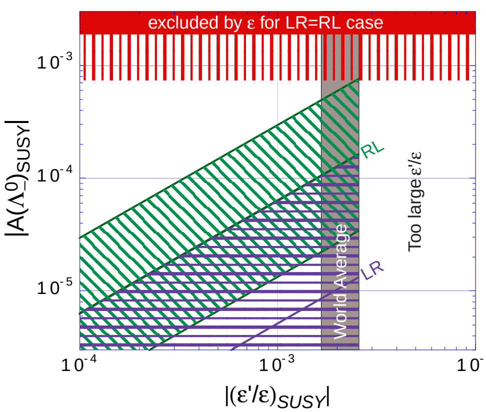

Fig. 12. The allowed regions on $(|(\varepsilon'/\varepsilon)_{\mathrm{SUSY}}|,\ |A(\Lambda^0_-)_{\mathrm{SUSY}}|)$ parameter space for three cases: (a) only $\mathrm{Im}(\delta^d_{12})_{\mathrm{LR}}$ contribution, which is the conservative case (hatched horizontally), (b) only $\mathrm{Im}(\delta^d_{12})_{\mathrm{RL}}$ contribution (hatched diagonally), and (c) $\mathrm{Im}(\delta^d_{12})_{\mathrm{LR}} = \mathrm{Im}(\delta^d_{12})_{\mathrm{RL}}$ case which does not contribute to ε' and can give a large $|A(\Lambda^0_-)|$ below the shaded region (or vertically hatched region for the central values of the matrix elements). The last case is motivated by the relation $\lambda = \sqrt{m_d/m_s}$. The vertical shaded band is the world average [70] of ε'/ε. The region to the right of the band is therefore not allowed.

a large ε' [71], but $A(\Lambda^0_-)$ is small as in the 3-Higgs model of [43]. However, in models in which $\mathrm{Im}(\delta^d_{12})_{\mathrm{LR}} = \mathrm{Im}(\delta^d_{12})_{\mathrm{RL}}$ the CP-violating operator is parity-even. In this case there is no contribution to ε' and $A(\Lambda^0_-)$ can be as large as 10^{-3} [48]. It is interesting that this type of model is not an ad-hoc model to give a large $A(\Lambda^0_-)$, but is a type of model originally designed to naturally reproduce the relation $\lambda = \sqrt{m_d/m_s}$, as in Ref. [73], for example.

3.6. Conclusion and comments on hyperon decay

E871 is expected to reach a sensitivity of 10^{-4} for the observable $A(\Lambda^0_-)+A(\Xi^-_-)$. I conclude that a non-zero measurement by E871 is not only possible but that it would provide valuable complementary information to what we already know from ε'. It would almost certainly indicate physics beyond the standard model.

Finally I would like to mention two related issues. A search for $\Delta S = 2$ hyperon non-leptonic decays is also a useful enterprise as it provides information that is complementary to what we know from $K - \bar{K}$ mixing [74]. A CP-violating rate asymmetry in $\Omega \to \Xi\pi$ decay can be as large as 2×10^{-5} within the standard model (and up to ten times larger beyond), much larger than the corresponding rate asymmetries in octet-hyperon decay [75].

This work was supported in part by DOE under Contract Number DE-FG02-01ER41155. I wish to thank the organizers of the School and in particular Michał Praszałowicz for a very stimulating meeting and warm hospitality.

REFERENCES

[1] C. Jarlskog, not submitted to the Proceedings.

[2] N. Cabibbo, *Phys. Rev. Lett.* **10**, 531 (1963); M. Kobayashi, T. Maskawa, *Prog. Theor. Phys.* **49**, 652 (1973).

[3] L. Wolfenstein, *Phys. Rev. Lett.* **51**, 1945 (1983).

[4] H. Leutwyler, M. Roos, *Z. Phys.* **C25**, 91 (1984).

[5] K. Hagiwara *et al.* [Particle Data Group Collaboration], *Phys. Rev.* **D66**, 010001 (2002).

[6] Some reviews of this and other kaon decay modes are J.L. Ritchie, S.G. Wojcicki, *Rev. Mod. Phys.* **65**, 1149 (1993); L. Littenberg, G. Valencia, *Annu. Rev. Nucl. Part. Sci.* **43**, 729 (1993); G. D'Ambrosio, G. Isidori, *Int. J. Mod. Phys.* **A13**, 1 (1998); A.R. Barker, S.H. Kettell, *Annu. Rev. Nucl. Part. Sci.* **50**, 249 (2000).

[7] G. Buchalla, A. Buras, M. Harlander, *Nucl. Phys.* **B337**, 313 (1990); G. Buchalla, A.J. Buras, M.E. Lautenbacher, *Rev. Mod. Phys.* **68**, 1125 (1996).

[8] L.S. Littenberg, G. Valencia, *Phys. Lett.* **B385**, 379 (1996).

[9] S. Adler *et al.* [E787 Collaboration], *Phys. Rev. Lett.* **88**, 041803 (2002).

[10] A. Alavi-Harati, *et al.* [KTeV Collaboration], *Phys. Rev.* **D61**, 072006 (2000).

[11] Y. Grossman, Y. Nir, *Phys. Lett.* **B398**, 163 (1997).

[12] G. Valencia, *Nucl. Phys.* **B517**, 339 (1998).

[13] J. Gasser, H. Leutwyler, *Nucl. Phys.* **B250**, 465 (1985).

[14] J.A. Cronin, *Phys. Rev.* **161**, 1483 (1967).

[15] J. Kambor, J. Missimer, D. Wyler, *Phys. Lett.* **B261**, 496 (1991).

[16] G.D. Barr *et al.* [NA31 Collaboration], *Phys. Lett.* **B242**, 523 (1990); **B284**, 440 (1992); **B328**, 528 (1994); V. Papadimitriou *et al.* [E731 Collaboration], *Phys. Rev.* **D44**, 573 (1991).

[17] L. Cappiello, G. D'Ambrosio, M. Miragliuolo, *Phys. Lett.* **B298**, 423 (1993).

[18] A.G. Cohen, G. Ecker, A. Pich, *Phys. Lett.* **B304**, 347 (1993).

[19] G. Ecker, A. Pich, E. de Rafael, *Phys. Lett.* **B237**, 481 (1990).

[20] G. Ecker, A. Pich, E. de Rafael, *Nucl. Phys.* **B303**, 665 (1988).

[21] G. Ecker, A. Pich, E. de Rafael, *Phys. Lett.* **B189**, 363 (1987); L. Cappiello, G. D'Ambrosio, *Nuovo Cim.* **A99**, 153 (1988).

[22] J.F. Donoghue, E. Golowich, B.R. Holstein, *Phys. Rev.* **D30**, 587 (1984).

[23] A. Alavi-Harati *et al.* [KTeV Collaboration], *Phys. Rev. Lett.* **83**, 917 (1999).

[24] J. Bijnens, S. Dawson, G. Valencia, *Phys. Rev.* **D44**, 3555 (1991); M. Praszalowicz, G. Valencia, *Nucl. Phys.* **B341**, 27 (1990).

[25] L.M. Sehgal, *Phys. Rev.* **D41**, 161 (1990); P. Ko, J.L. Rosner, *Phys. Rev.* **D40**, 3775 (1989); P. Ko, *Phys. Rev.* **D41**, 1531 (1990).

[26] F. Gabbiani, G. Valencia, *Phys. Rev.* **D64**, 094008 (2001).

[27] F. Gabbiani, G. Valencia, `hep-ph/0207189`, accepted for publication in *Phys. Rev.* **D**.

[28] S. Fajfer, *Phys. Rev.* **D51**, 1101 (1995); *Nuovo Cim.* **A109**, 1439 (1996).

[29] J.F. Donoghue, C. Ramirez, G. Valencia, *Phys. Rev.* **D39**, 1947 (1989).

[30] P. Astier *et al.* [NOMAD Collaboration], *Nucl. Phys.* **B601**, 3 (2001).

[31] H. Marsike *et al.* [Crystal Ball Collaboration], *Phys. Rev.* **D41**, 3324 (1990).

[32] H. Pilkuhn, *The Interactions of Hadrons*, J. Wiley & Sons, New York 1967.

[33] A. Lai *et al.* [NA48 Collab.], *Phys. Lett.* **B536**, 229 (2002).

[34] J.F. Donoghue, B.R. Holstein, G. Valencia, *Phys. Rev.* **D35**, 2769 (1987).

[35] J.F. Donoghue, F. Gabbiani, *Phys. Rev.* **D51**, 2187 (1995); *Phys. Rev.* **D56**, 1605 (1997).

[36] G.J. Feldman, R.D. Cousins, *Phys. Rev.* **D57**, 3873 (1998).

[37] J. Bijnens, P. Dhonte, F. Persson, `hep-ph/0205341`.

[38] S. Okubo, *Phys. Rev.* **109**, 984 (1958); A. Pais, *Phys. Rev. Lett.* **3**, 242 (1959).

[39] K.B. Luk *et al.* [E756 Collaboration], *Phys. Rev. Lett.* **85**, 4860 (2000).

[40] K.B. Luk *et al.* [E756 Collaboration], `hep-ex/0005004`.

[41] O.E. Overseth, *Phys. Lett.* **111B**, 286 (1982).

[42] L.D. Roper, R.M. Wright, B. Feld, *Phys. Rev.* **138**, 190 (1965); A. Datta, S. Pakvasa, *Phys. Rev.* **D56**, 4322 (1997).

[43] J. Donoghue, S. Pakvasa, *Phys. Rev. Lett.* **55**, 162 (1985); J. Donoghue, X.-G. He, S. Pakvasa, *Phys. Rev.* **D34**, 833 (1986).

[44] X.-G. He, H. Steger, G. Valencia, *Phys. Lett.* **B272**, 411 (1991).

[45] M.J. Iqbal, G.A. Miller, *Phys. Rev.* **D41**, 2817 (1990).

[46] X.-G. He, G. Valencia, *Phys. Rev.* **D52**, 5257 (1995).

[47] D. Chang, X.-G. He, S. Pakvasa, *Phys. Rev. Lett.* **74**, 3927 (1995).

[48] Xiao-Gang He, H. Murayama, S. Pakvasa, G. Valencia, *Phys. Rev.* **D61**, 071701 (2000).

[49] M. Lu, M. Savage, M. Wise, *Phys. Lett.* **B337**, 133 (1994).

[50] A. Datta, S. Pakvasa, *Phys. Lett.* **B344**, 430 (1995).

[51] A. Kamal, *Phys. Rev.* **D58**, 077501 (1998).

[52] J. Tandean, A.W. Thomas, G. Valencia, *Phys. Rev.* **D64**, 014005 (2001).

[53] U.-G. Meissner, J.A. Oller, *Phys. Rev.* **D64**, 014006 (2001).

[54] N. Kaiser, *Phys. Rev.* **C64**, 045204 (2001).

[55] J. Bijnens, H. Sonoda, M.B. Wise, *Nucl. Phys.* **B261**, 185 (1985).

[56] H. Georgi, *Weak Interactions and Modern Particle Theory*, The Benjamin/Cummings Publishing Company, Menlo Park 1984.

[57] J.F. Donoghue, E. Golowich, B.R. Holstein, *Dynamics of the Standard Model*, Cambridge University Press, Cambridge 1992.

[58] E. Jenkins, A. Manohar, in *Effective Field Theories of the Standard Model*, edited by U.-G. Meissner, World Scientific, Singapore 1992.

[59] E. Jenkins, A.V. Manohar, *Phys. Lett.* **B255**, 558 (1991).

[60] E. Jenkins, A. Manohar, *Phys. Lett.* **B259**, 353 (1991).

[61] A. Abd El-Hady, J. Tandean, G. Valencia, *Nucl. Phys.* **A651**, 71 (1999).

[62] N. Kaiser, P.B. Siegel, W. Weise, *Nucl. Phys.* **A594**, 325 (1995); N. Kaiser, T. Waas, W. Weise, *Nucl. Phys.* **A612**, 297 (1997); J. Caro Ramon, N. Kaiser, S. Wetzel, W. Weise, *Nucl. Phys.* **A672**, 249 (2000); C.H. Lee, G.E. Brown, D.-P. Min, M. Rho, *Nucl. Phys.* **A585**, 401 (1995); J.W. Bos *et al.*, *Phys. Rev.* **D51**, 6308 (1995); **57**, 4101 (1998); G. Müller, U.-G. Meissner, *Nucl. Phys.* **B492**, 379 (1997).

[63] E. Jenkins, *Nucl. Phys.* **B375**, 561 (1992).

[64] A. Hocker, H. Lacker, S. Laplace, F. Le Diberder, *Eur. Phys. J.* **C21**, 225 (2001).

[65] R.P. Springer, `hep-ph/9508324`; *Phys. Lett.* **B461**, 167 (1999); B. Borasoy, B.R. Holstein, *Phys. Rev.* **D59**, 094025 (1999).

[66] A. Abd El-Hady, J. Tandean, *Phys. Rev.* **D61**, 114014 (2000).

[67] B. Borasoy, B.R. Holstein, *Phys. Rev.* **D59**, 094025 (1999).

[68] J. Tandean, G. Valencia, in preparation.

[69] S. Chivukula, J. Flynn, H. Georgi, *Phys. Lett.* **B171**, 453 (1986). A recent review can be found in E. de Rafael, TASI 94 lectures, `hep-ph/9502254`.

[70] This is the average of E731, NA31, KTeV and NA48 with the error bar inflated to obtain $\chi^2/\text{d.o.f.} = 1$ according to the Particle Data Group prescription.

[71] A. Masiero, H. Murayama, *Phys. Rev. Lett.* **83**, 907 (1999).

[72] F. Gabbiani, *et. al.*, *Nucl. Phys.* **B447**, 321 (1996).

[73] R. Barbieri, G. Dvali, L.J. Hall, *Phys. Lett.* **B377**, 76 (1996).

[74] X.-G. He, G. Valencia, *Phys. Lett.* **B409**, 469 (1997), Erratum-ibid. **B418**, 443 (1998).

[75] J. Tandean, G. Valencia, *Phys. Lett.* **B451**, 382 (1999).